

## REPORT 1063

# AIRFOIL PROFILES FOR MINIMUM PRESSURE DRAG AT SUPERSONIC VELOCITIES—GENERAL ANALYSIS WITH APPLICATION TO LINEARIZED SUPERSONIC FLOW<sup>1</sup>

By DEAN R. CHAPMAN

### SUMMARY

A theoretical investigation is made of the airfoil profile for minimum pressure drag at zero lift in supersonic flow. In the first part of the report a general method is developed for calculating the profile having the least pressure drag for a given auxiliary condition, such as a given structural requirement or a given thickness ratio. The various structural requirements considered include bending strength, bending stiffness, torsional strength, and torsional stiffness. No assumption is made regarding the trailing-edge thickness; the optimum value is determined in the calculations as a function of the base pressure.

To illustrate the general method, the optimum airfoil, defined as the airfoil having minimum pressure drag for a given auxiliary condition, is calculated in a second part of the report using the equations of linearized supersonic flow. It is found that the optimum airfoil in most cases has a blunt trailing edge. It also is found that the optimum thickness distribution depends only on one dimensionless parameter, termed the "base pressure parameter". This parameter involves the Mach number, airfoil thickness ratio, and base pressure coefficient. The effect of variations in each of these latter three quantities on the shape of the optimum profile is discussed, and a simple criterion formulated for determining the condition under which the optimum trailing-edge thickness is greater than zero. The calculated pressure drag of the optimum profile is compared to that of a biconvex sharp-trailing-edge profile satisfying the same structural requirement. The reduction in pressure drag depends on the base pressure parameter and varies from a few percent to as much as 75 percent.

### INTRODUCTION

In supersonic flow the finite thickness of an airfoil invariably introduces a certain amount of pressure drag which can be minimized by a rational choice of airfoil shape. The profile for minimum pressure drag depends, among other things, on the particular auxiliary condition that is imposed on the airfoil geometry. For example, if it is required that the optimum profile (defined herein as the profile of least pressure drag for a given auxiliary condition) satisfy the auxiliary condition of a given thickness ratio, then according to a well-known result of Ackeret's linearized airfoil theory, the so-called double-wedge profile represents the optimum

sharp-trailing-edge airfoil. This particular auxiliary condition, however, does not represent practical cases where an airfoil must satisfy a certain structural requirement, such as a given area moment of inertia, or a given section modulus. Drougge (reference 1) has made a more elaborate theoretical analysis to determine the optimum profile for the auxiliary condition of a given bending stiffness of the airfoil, and also for the condition of a given torsional stiffness. Drougge used linearized airfoil theory and considered only sharp-trailing-edge airfoils. His results are somewhat limited in two respects: They do not cover cases outside the scope of linearized airfoil theory, and, though they include the auxiliary conditions of given bending and torsional stiffness, they do not include the auxiliary condition of a given bending strength (given section modulus). A far more important limitation of this analysis, though, is the tacit assumption that the optimum airfoil will have a sharp trailing edge.

There is a small amount of experimental evidence in the measurements of Ferri (reference 2) on airfoils with sharp trailing edges which suggests that the optimum airfoil might, in fact, have a moderately thick trailing edge. The measured profile drag of one airfoil tested by Ferri (G. U. 3 airfoil at a Mach number of 1.85) was considerably lower than inviscid theory would indicate. Allowance for skin friction would cause this discrepancy to become even greater. Schlieren photographs and pressure-distribution measurements showed that viscous effects effectively thickened the airfoil shape near the trailing edge. From these results it can be inferred that at moderate supersonic velocities it is possible for an airfoil with a thickened trailing edge—that is, a blunt-trailing-edge airfoil—to have lower drag than a corresponding sharp-trailing-edge airfoil. Employing a different approach, this inference has been obtained from quantitative considerations in reference 3, where a reasonable estimate of the base pressure was made and the drag calculated as a function of trailing-edge thickness. Such calculations, though very approximate, have indicated that in certain cases a moderate increase in trailing-edge thickness will decrease the over-all pressure drag.

Apart from the reasons just cited for expecting that the optimum supersonic airfoil might have a thick trailing edge, there are other independent considerations which suggest

<sup>1</sup>Supersedes NACA TN 2264, "Airfoil Profiles for Minimum Pressure Drag at Supersonic Velocities—General Analysis With Application to Linearized Supersonic Flow," by Dean R. Chapman, 1951. Various examples of optimum profiles given in TN 2264 have been supplemented and revised for the present report in accordance with experimental measurements of base pressure published subsequent to TN 2264.

the same result. By analyzing conditions at infinite Mach number, Saenger pointed out in 1933 that even with a vacuum at the base the optimum airfoil for a given thickness ratio would, in this extreme case, have a trailing-edge thickness equal to the maximum airfoil thickness. (See reference 4.) In reference 5, Ivey obtained a similar result by calculating the pressure drag at a Mach number of 8 for a family of airfoils having various positions of maximum thickness. More recently, Smelt (reference 6) has developed an approximate condition determining when an airfoil with maximum thickness at the trailing edge has lower drag in hypersonic flow than an airfoil with a sharp trailing edge. Saenger, Ivey, and Smelt, however, did not consider airfoils having a trailing-edge thickness less than the maximum airfoil thickness, and hence their results do not determine the optimum profile for hypersonic velocities. Nevertheless, it is evident that at high supersonic Mach numbers the optimum profile has a relatively thick trailing edge. On this basis it is not unreasonable to expect that at lower supersonic Mach numbers the optimum profile would have some thickness at the trailing edge.

The physical reason why it is possible for a blunt-trailing-edge airfoil in supersonic flow to have a lower pressure drag than a corresponding sharp-trailing-edge airfoil is quite simple, as can be illustrated by the two profiles shown in figure 1. These profiles have the same area, which corresponds to the same torsional stiffness of a thin-skin structure

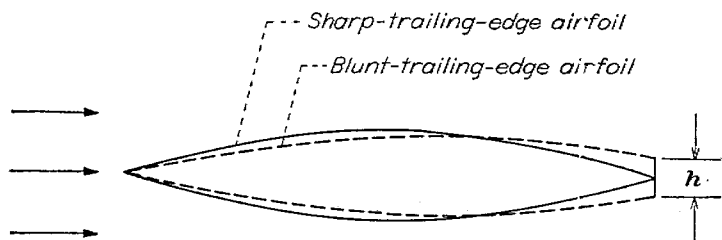


FIGURE 1.—Sketch comparing a typical sharp-trailing-edge airfoil and a blunt-trailing-edge airfoil of equal area (equal torsional stiffness for a thin-skin structure).

The blunt-trailing-edge airfoil has a slightly smaller thickness ratio and a position of maximum thickness which is farther rearward, hence the leading-edge angle is smaller and the pressure drag of the surface forward of the trailing edge is less than that of the sharp-trailing-edge airfoil. A certain amount of base drag, however, obviously is added by employing a thick trailing edge. If the added base drag is less than the reduction in pressure foredrag, then the net result is a smaller total pressure drag for the blunt-trailing-edge airfoil. This invariably is the case at extremely high supersonic Mach numbers where the base drag is negligible compared to the pressure foredrag. At low supersonic Mach numbers, though, the base drag can be many times the pressure foredrag, and the optimum trailing-edge thickness must be expected a priori to depend to a great extent on the base pressure.

The present theoretical analysis was initiated in view of the foregoing considerations. The primary purpose of the investigation is to develop a method of determining the supersonic airfoil profile for minimum pressure drag at zero lift, without making an arbitrary assumption about the trail-

ing-edge thickness. The profile so determined, which is termed an optimum profile, is considered to depend on the base pressure, Mach number, and the particular auxiliary condition imposed on the airfoil. A secondary purpose of the investigation is to develop a method of sufficient generality to enable second-order and shock expansion theories to be used in calculating optimum profiles. Such generality is desirable in order to obtain results that are valid at hypersonic Mach numbers.

#### NOTATION

$B$	base pressure parameter for linearized supersonic flow $\left[ \frac{-P_b}{(t/c) \sqrt{M_\infty^2 - 1}} \right]$
$\bar{B}$	limiting value of the base pressure parameter below which the optimum airfoil has a blunt trailing edge
$c$	airfoil chord
$c_d$	section pressure drag coefficient
$f$	symbol for the function $P_y'$
$F(k, \varphi)$	incomplete elliptic integral of the first kind of modulus $k$ and amplitude $\varphi$
$h$	trailing-edge thickness
$H$	dimensionless trailing-edge thickness ( $h/t$ )
$I$	given value of the auxiliary integral $\left[ \frac{1}{c} \int_0^c \frac{y^n}{(t/2)^\sigma} dx \right]$
$k_n$	constant defined by equation (20)
$l$	length of chord over which airfoil thickness is constant
$L$	dimensionless length of chord over which airfoil thickness is constant ( $l/s$ )
$M$	Mach number
$n$	arbitrary parameter appearing in the definition of the auxiliary integral $I$ (For the examples considered $n$ is taken as 1, 2, 3 or $\infty$ .)
$p$	static pressure on airfoil surface
$P$	pressure coefficient $\left[ (p - p_\infty) / \left( \frac{1}{2} \rho_\infty V_\infty^2 \right) \right]$
$P_b$	base pressure coefficient $\left[ (p_b - p_\infty) / \left( \frac{1}{2} \rho_\infty V_\infty^2 \right) \right]$
$Re$	Reynolds number based on airfoil chord
$s$	distance from leading edge to first downstream position of maximum thickness
$t$	maximum thickness of airfoil
$V$	velocity
$x$	distance from leading edge
$X$	dimensionless distance from leading edge ( $x/s$ )
$y$	ordinate of upper half of airfoil
$Y$	dimensionless ordinate [ $y/(t/2)$ ]
$\beta$	$\sqrt{M_\infty^2 - 1}$
$\lambda$	Langrangian multiplier (arbitrary constant)
$\sigma$	arbitrary parameter appearing in the definition of the auxiliary integral $I$ (For the examples considered $\sigma$ is taken as 0 or 1.)
$\rho$	mass density

#### SUBSCRIPTS

0	airfoil surface at leading edge
1	airfoil surface at trailing edge
$\infty$	free stream
$b$	base

- ca* circular-arc biconvex airfoil with sharp trailing edge
- dw* double-wedge airfoil with sharp trailing edge
- v* vacuum at base

SUPERSCRIPT

' differentiation with respect to *x*

THEORETICAL ANALYSIS

ASSUMPTIONS AND STATEMENT OF PROBLEM

In the analysis which follows several simplifying assumptions are made. Two-dimensional airfoils in a purely supersonic flow at zero lift only are considered. It is assumed that the pressure at any point on the airfoil surface forward of the trailing edge can be calculated from the flow of an inviscid, nonconducting gas. It is further assumed that the leading edge is sharp. No analogous assumption is made regarding the trailing-edge thickness, but it is assumed that the base pressure coefficient *P<sub>b</sub>* is known. This enables the optimum trailing-edge thickness to be calculated as a function of *P<sub>b</sub>*; hence, experimental data on base pressure in two-dimensional flow are required in order to apply the theoretical results of the analysis to a given case.

From the fact that the surface pressures on the top and bottom of an airfoil can be calculated independently in a supersonic flow, it follows that at zero lift the optimum profile will be symmetrical about the chord plane. Consequently, reference is made throughout to the thickness distribution of only the upper surface of an optimum profile.

In comparing the pressure drag of various profiles, the chord length is held constant, and the thickness distribution along the chord is varied in a manner which is arbitrary except for the requirement of satisfying the particular auxiliary condition being considered. The various auxiliary conditions investigated are: a given torsional stiffness of the airfoil section, a given torsional strength, a given bending stiffness, a given bending strength, and a given thickness ratio. For each of the structural conditions the case of a thin-skin structure and a solid-section structure is considered since the optimum airfoil profile may be expected to depend somewhat on the type of structure. Attention is focused on the fact that the basic idea employed in the analysis involves the minimizing of pressure drag for a given structural requirement; the results obtained with this method of approach are the same as would be obtained if the structural characteristic were maximized for a given value of the drag.<sup>2</sup>

MATHEMATICAL FORMULATION OF PROBLEM

The pressure drag *c<sub>d</sub>* of an airfoil with a thick trailing edge is the sum of the base drag and the pressure drag of the surface forward of the trailing edge. Letting *P* be the surface pressure coefficient, *y(x)* the function defining the surface, and *P<sub>b</sub>* the base pressure coefficient, then *c<sub>d</sub>* may be expressed as

$$c_d = \frac{2}{c} \int_0^c P y' dx - P_b \frac{h}{c} \tag{1}$$

The problem is to determine the particular function *y(x)* and the corresponding value of the trailing-edge thickness

*h* which minimizes this expression for a given auxiliary condition.

Before expressing the various auxiliary conditions in analytical form, it should be noted that the surface pressure coefficient *P* is regarded as a known function of the variable *y'* and the two parameters *y'<sub>0</sub>* (surface slope at leading edge) and *M<sub>∞</sub>*. The actual functional form of *P(y', y'<sub>0</sub>, M<sub>∞</sub>)* will depend on whether linearized, second-order, hypersonic, or shock-expansion theory is employed in calculating surface pressures. For example, if linear theory were employed, the explicit expression  $P = 2y' / \sqrt{M_\infty^2 - 1}$  would be used; but, if shock-expansion theory were employed, a more complex implicit expression involving *y'<sub>0</sub>* as well as *y'* and *M<sub>∞</sub>* would have to be used. In order to allow various theories to be employed, the particular functional form of *P(y', y'<sub>0</sub>, M<sub>∞</sub>)* will at present be unspecified. The equations which result can be applied to any of the various theories by substituting the appropriate function for *P*.

Turning now to the consideration of auxiliary conditions, it is clear that some integral expression will be involved, since the function *y(x)* is not known beforehand. If, for example, the airfoil is a solid-section structure and the moment of inertia is prescribed, then the particular auxiliary condition which *y(x)* must satisfy in addition to minimizing *c<sub>d</sub>* is that the integral  $\int_0^c y^3 dx$  be constant. A different auxiliary condition would, of course, be represented by a different integral. In the present investigation a somewhat generalized auxiliary condition is used which is represented by the single integral

$$I = \frac{1}{c} \int_0^c \frac{y^n}{(t/2)^\sigma} dx = \text{constant} \tag{2}$$

where *n* and *σ* are constants. Thus the example just cited is a special case of the above integral with *n*=3 and *σ*=0. To illustrate further, the auxiliary condition of a given section modulus of a solid-section airfoil is represented by the special case *n*=3 and *σ*=1. The corresponding solution for *y(x)* in this latter case would provide the profile of least pressure drag for a given bending strength.

Some of the different structural criteria to which the general integral (2) corresponds are summarized in the following table:<sup>3</sup>

<i>n</i>	<i>σ</i>	Structural criteria
1	0	Given torsional stiffness, or torsional strength, or volume of thin-skin structure
2	0	Given bending stiffness of thin-skin structure
3	0	Given bending stiffness or given torsional stiffness of solid-section structure*
2	1	Given bending strength of thin-skin structure
3	1	Given bending strength of solid-section structure

\* As a first approximation the torsional stiffness of a thin solid-section profile is taken to be proportional to the moment of inertia about the chord plane.

Thus, by solving the problem with the general integral (2) left in terms of *n* and *σ* a wide variety of auxiliary con-

<sup>2</sup> This statement, which appears evident from physical considerations, is equivalent to Mayer's reciprocity theorem for isoperimetric problems in the calculus of variations.  
<sup>3</sup> For thin-skin structures the thickness of skin is taken to be constant over the chord length. The two cases *n*=*σ*=0 and *n*=*σ*=1 are not included in this table as they apparently represent no sensible practical problem.

ditions can be obtained simply by substituting appropriate integers for  $n$  and  $\sigma$ . From an engineering viewpoint the general form of equation (2) enables approximate solutions to be obtained for wings of intermediate structural solidity by interpolating between the solution for essentially zero solidity (thin-skin structures) and the solution for complete solidity (solid-section structure).

Summarizing, the problem formulated can be stated mathematically as that of finding the airfoil-ordinate function  $y(x)$ , and the trailing-edge thickness  $h=y(c)$ , which minimizes the drag expression (1) for a given constant value of the structural integral (2). The boundary conditions imposed are that  $y(0)=0$  and that  $P_b$  is given. If  $t$  did not appear in equation (2), this mathematical problem would be a relatively simple isoperimetric problem in the calculus of variations. The occurrence of  $t$ , the maximum value of  $y(x)$ , complicates matters because it is not known beforehand and, in fact, is one of the quantities to be determined from the given values of  $M_\infty$ ,  $P_b$ , and  $I$ . Actually, all equations necessary for solving the problem formulated could be obtained directly from advanced treatises on the calculus of variations since the problem is a special case of the so-called "problem of Bolza with variable end points". (Such a procedure would lead quickly to equations (11), (12), and (13).) However, the necessary equations can also be obtained by the simple methods employed here.

METHOD OF SOLUTION

**Given structural criteria.**—Since the pressure drag of the optimum airfoil, by definition, is the least possible of all airfoils having a given value of the structural integral (2), it follows that the pressure drag of any "varied" airfoil, having ordinates and slopes everywhere close to those of the optimum airfoil, must be in the neighborhood of a minimum. Hence, by considering only infinitesimal changes  $\delta y$  in the ordinate of the optimum profile, the corresponding increment in drag  $\delta c_d$  of such a varied profile can be equated to zero. Since  $y(x)$  is to provide the true minimum, the resulting equation must hold for an arbitrary ordinate change  $\delta y$  varying with  $x$ , or for an arbitrary change in airfoil thickness  $\delta t$ , or for an arbitrary change in trailing-edge thickness  $\delta h$ , or for any combination of variations thereof, provided only that the integral (2) is constant for all such variations.

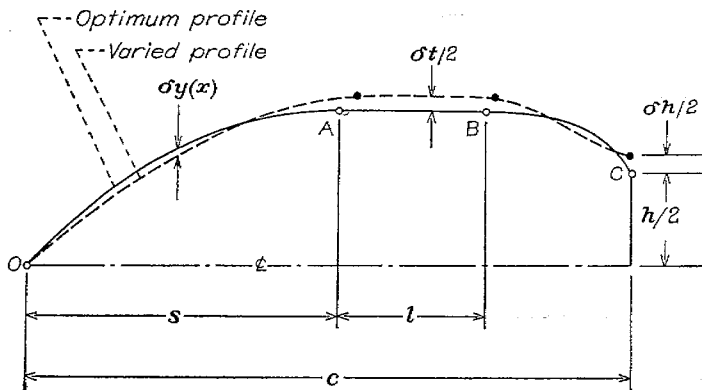


FIGURE 2.—Sketch of upper half of varied and optimum profiles.

Application of this basic principle, as will be seen, leads to a sufficient number of equations to determine the complete geometry of the optimum profile.

A sketch of the type of optimum profile to be analyzed and the corresponding varied profile is shown in figure 2. Various quantities which appear often in the subsequent analysis are illustrated in this figure. It is to be noted that allowance is made for the possibility that the optimum profile may have a straight midsection of length  $l$ , the optimum value of which must be determined from the analysis. The varied profile is selected such that it does not change the ordinate or the surface slope at the leading edge. Introducing the definition  $f \equiv Py'$  for the purpose of brevity, and equating the drag of the optimum profile to the drag of the infinitesimally varied profile, yields

$$\int_0^c f dx - P_b \frac{h}{2} = \frac{c}{2} c_d = \int_0^c \left( f + \frac{\partial f}{\partial y'} \delta y' \right) dx - P_b \frac{h + \delta h}{2} \quad (3)$$

The small change in slope  $\delta y'$  is equal to  $\frac{d}{dx} (\delta y)$ , so equation (3) can be written

$$0 = \int_0^c \frac{\partial f}{\partial y'} \frac{d(\delta y)}{dx} dx - P_b \frac{\delta h}{2} \quad (4)$$

Integrating by parts,

$$\begin{aligned} 0 &= \frac{\partial f}{\partial y'} \delta y \Big|_{x=0}^{x=c} - \int_0^c \delta y \frac{d}{dx} \left( \frac{\partial f}{\partial y'} \right) dx - P_b \frac{\delta h}{2} \\ &= \left( \frac{\partial f}{\partial y'} \right)_1 \frac{\delta h}{2} - \int_0^c \delta y \frac{d}{dx} \left( \frac{\partial f}{\partial y'} \right) dx - P_b \frac{\delta h}{2} \end{aligned}$$

or, finally

$$\delta c_d = 0 = - \int_0^c \delta y \frac{d}{dx} \left( \frac{\partial f}{\partial y'} \right) dx + \left[ \left( \frac{\partial f}{\partial y'} \right)_1 - P_b \right] \frac{\delta h}{2} \quad (5)$$

The chordwise distribution of the variation  $\delta y$  is not entirely arbitrary; it must be such that the auxiliary condition is satisfied, namely, the value of  $I$  for the optimum profile must be equal to that of the varied profile.

$$\frac{1}{c} \int_0^c \frac{y^n}{(t/2)^\sigma} dx = I = \frac{1}{c} \int_0^c \frac{(y + \delta y)^n}{(t/2 + \delta t/2)^\sigma} dx \quad (6)$$

Retaining only first order variations, this expression simplifies to

$$\int_0^c y^n dx = \int_0^c y^n dx + \int_0^c n y^{n-1} \delta y dx - \sigma \frac{\delta t}{t} \int_0^c y^n dx \quad (7)$$

or

$$0 = \int_0^c n y^{n-1} \delta y dx - \sigma c I \left( \frac{t}{2} \right)^\sigma \frac{\delta t}{t} \quad (8)$$

This equation must be satisfied, of course if both terms on the right side are multiplied by an arbitrary constant  $\lambda$ . Moreover, equation (5) must be satisfied simultaneously. The arbitrary character of  $\lambda$  enables the two equations (5) and (8) to be combined into a single equation which must hold for arbitrary variations in  $\delta y$ ,  $\delta h$ , and  $\delta t$ .

$$0 = - \int_0^c \delta y \left[ + \frac{d}{dx} \left( \frac{\partial f}{\partial y'} \right) + \lambda n y^{n-1} \right] dx + \left[ \left( \frac{\partial f}{\partial y'} \right)_1 - P_b \right] \frac{\delta h}{2} + \lambda \sigma c I \left( \frac{t}{2} \right)^\sigma \frac{\delta t}{t} \quad (9)$$

Thus, since  $\lambda$  is arbitrary, this single equation implies that both equations (5) and (8) are satisfied.

If at this point the variation  $\delta t$  is considered to be arbitrary, equation (9) as written would incorrectly suggest that  $\lambda \sigma c I$  must be zero. Hence it is to be expected that an additional term containing  $\delta t$  exists in the integral expression of equation (9). Such a term arises from the contribution of the straight midsection to this integral, since over this region,  $\delta y = \delta t/2$ . Also,  $y = t/2$  and  $\frac{d}{dx} \left( \frac{\partial f}{\partial y'} \right) = 0$  over this region. Hence

$$0 = - \int_0^s \delta y \left[ + \frac{d}{dx} \left( \frac{\partial f}{\partial y'} \right) + \lambda n y^{n-1} \right] dx - \int_{s+l}^c \delta y \left[ + \frac{d}{dx} \left( \frac{\partial f}{\partial y'} \right) + \lambda n y^{n-1} \right] dx + \left[ \left( \frac{\partial f}{\partial y'} \right)_1 - P_b \right] \frac{\delta h}{2} + \lambda \left[ -n \left( \frac{t}{2} \right)^{n-1} l + \sigma c I \left( \frac{t}{2} \right)^{\sigma-1} \right] \frac{\delta t}{2} \quad (10)$$

The variations  $\delta y$ ,  $\delta h$ , and  $\delta t$  can now be conducted entirely independent of each other. Each of the bracketed terms in equation (10) must be zero, if the individual variations are not zero. Reemploying the definition  $f = P y'$ , the following equations are obtained:

for  $\delta y \neq 0$

$$\frac{d}{dx} \left( P + y' \frac{\partial P}{\partial y'} \right) + \lambda n y^{n-1} = 0 \quad (11)$$

for  $\delta h \neq 0$

$$P_1 + \left( y' \frac{\partial P}{\partial y'} \right)_1 - P_b = 0 \quad (12)$$

for  $\lambda \delta t \neq 0$

$$n \frac{l}{c} - \sigma \frac{I}{(t/2)^{n-\sigma}} = 0 \quad (13)$$

The differential equation (11), of course, results from equating to zero each of the two integrals in equation (10). This differential equation, therefore, need be satisfied only in the two chordwise regions covered by the limits of these integrals, namely, in the region from  $x=0$  to  $x=s$ , and in the region from  $x=s+l$  to  $x=c$ . (See fig. 2.) If the optimum airfoil has a finite length of straight midsection (e.g., AB in fig. 2), the differential equation (11) need not be satisfied in this intermediate region.

Fortunately, one integration of equation (11) can immediately be made, thereby lowering the order of the basic differential equation to be solved. Multiplying equation (11) by  $y'$  gives

$$\begin{aligned} 0 &= y' \frac{d}{dx} \left( P + y' \frac{\partial P}{\partial y'} \right) + \lambda n y^{n-1} y' \\ &= 2 y' y'' \frac{\partial P}{\partial y'} + y'^2 y'' \frac{\partial^2 P}{\partial y'^2} + \lambda \frac{d}{dx} (y^n) \\ &= \frac{d}{dx} \left( y'^2 \frac{\partial P}{\partial y'} + \lambda y^n \right) \end{aligned}$$

From this it is seen that a first integral of the basic differential equation (11) is

$$y'^2 \frac{\partial P}{\partial y'} + \lambda y^n = \text{constant} \quad (11a)$$

At the point, or points, where  $y' = 0$  the ordinate is equal to  $t/2$ . Evaluating the constant of equation (11a) from this consideration yields

$$y'^2 \frac{\partial P}{\partial y'} = \lambda [(t/2)^n - y^n] \quad (11b)$$

This equation, together with equation (12), equation (13), the given value of  $I$ , and the boundary condition  $y(0) = 0$ , determines the complete geometry of the optimum profile.

**Given thickness ratio.**—Attention is called to the fact that special precautions must be taken in applying the foregoing analysis to the auxiliary condition of a given thickness ratio. For this particular case  $\delta t$  is zero, thereby causing the last term in equation (10) to vanish automatically without requiring equation (13) to be satisfied; equation (13), therefore, does not necessarily apply when the thickness ratio is prescribed. Moreover, equation (11b) also does not necessarily apply since it was assumed in the process of obtaining this latter equation that the optimum airfoil had at least one point where  $y' = 0$ . Such is not the case for the auxiliary condition of a given thickness ratio, and hence more detailed consideration is required.

The appropriate differential equation to be used when  $t/c$  is given may be obtained from equation (11a)<sup>4</sup> by setting  $\lambda = 0$ . There results

$$y'^2 \frac{\partial P}{\partial y'} = \text{constant} \quad (14)$$

which is satisfied by any straight surface  $y' = \text{constant}$ , regardless of whether linearized, second-order, or shock-expansion theory is used for  $P$ . The appropriate condition which must be satisfied at the trailing edge is, from equation (10),

$$\left[ \left( P + y' \frac{\partial P}{\partial y'} \right)_1 - P_b \right] \delta h \geq 0 \quad (15)$$

Here the inequality is included since  $\delta h$  for the case of a given thickness ratio is not always entirely arbitrary. Thus, when  $h = t/2$  (wedge airfoil)  $\delta h$  is restricted to always be negative, and a minimum can exist if

$$\left[ P_1 + y'_1 \left( \frac{\partial P}{\partial y'} \right)_1 - P_b \right] < 0;$$

this would make  $\delta c_a$  always positive instead of just making  $c_a$  stationary. Consequently, under certain conditions two solutions are possible. First, the upper half of the optimum profile may consist of two straight segments with  $h < t$  (as illustrated in fig. 3), provided the equal sign in (15) applies. Second, the optimum profile may be a wedge profile with  $h = t$ , provided the inequality sign in (15) applies. If both types of solution are physically possible

<sup>4</sup> If equation (11) is used there results  $P + y' \frac{\partial P}{\partial y'} = \text{constant}$ , which also is satisfied by any straight surface. The constant in this latter equation, however, does not have the same value for both straight segments comprising the profile; whereas, the constant in equation (14) is the same for both segments. (See appendix.)

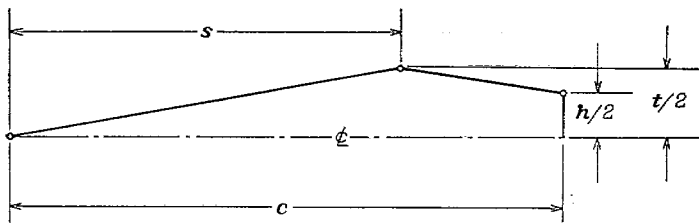


FIGURE 3.—Sketch of upper half of optimum profile for a given thickness ratio.

in a given case, the true solution, of course, would be the one with lower drag.

If it is possible to obtain a general solution to equations (11b), (12), and (13) (such is the case for linearized supersonic flow), then the first of the two solutions mentioned above may be obtained without solving equations (14) and (15), but by passing the general solution to the limit as  $n \rightarrow \infty$ .<sup>5</sup> In order to verify that this limiting condition represents the auxiliary condition of a given thickness ratio, three conditions must be satisfied: First, as  $n \rightarrow \infty$  the auxiliary integral must correspond to the case of a given thickness ratio; second, the differential equation (11b) must reduce to equation (14) in the limit as  $n \rightarrow \infty$ ; and third, the infinite value of  $n$  must be compatible with equation (13). Consider for the time being that the chord is of unit length. Since for any reasonable airfoil  $y < 1$ , it follows that  $\int_0^c y^n dx \rightarrow 0$  as  $n \rightarrow \infty$ , and hence  $I \rightarrow 0$ . A solution for  $I = 0$  would represent the optimum airfoil determined without regard for an auxiliary integral. Such is the condition that would be used in determining the optimum airfoil for a given thickness ratio; hence the first of the above-mentioned conditions is satisfied. Inasmuch as  $y/(t/2) < 1$ , it is evident that  $[y/(t/2)]^n \rightarrow 0$  as  $n \rightarrow \infty$ , thus reducing the differential equation (11b) to the form

$$y'^2 \frac{\partial P}{\partial y'} \rightarrow \lambda \left(\frac{t}{2}\right)^n = \text{constant}$$

which is the correct differential equation. As regards the third condition to be satisfied, it is seen that the values  $I = 0$ ,  $n = \infty$ ,  $l = 0$ , and  $\sigma = \text{finite}$  are compatible with equation (13). Consequently, the limiting case  $n \rightarrow \infty$  in the general solution to equations (11b), (12), and (13) represents one of the possible solutions for the case of a given thickness ratio. This fact will be used later in the report.

#### QUALITATIVE RESULTS OBTAINABLE WITHOUT SPECIALIZING TO A GIVEN TYPE OF SUPERSONIC FLOW

Although few quantitative results can be obtained from the basic systems of equations (11), (12), and (13), without specifying a particular form for the surface pressure coefficient  $P$ , there is one general qualitative result that can be obtained from equation (13) without any further calculation. The optimum length of straight midsection  $l$  always is zero for the auxiliary condition of a given torsional stiffness or a given bending stiffness ( $\sigma = 0$ ), but never is zero for the auxiliary condition of a given bending strength ( $\sigma = 1$ ). Since  $(t/2)^{n-\sigma}$  would be the value of  $I$  for a rectangular-bar airfoil of the

same thickness as the optimum airfoil, it is evident that for an actual airfoil  $I/(t/2)^{n-\sigma}$  will be of the order of one-half or two-thirds. As an example, this means that when bending strength is critical in a thin-skin structure ( $n = 2$ ), the optimum length of straight midsection will be of the order of one-third the chord length.

#### CALCULATION OF OPTIMUM PROFILES USING LINEAR AIRFOIL THEORY

##### SPECIALIZATION AND SOLUTION OF GENERAL EQUATIONS FOR LINEARIZED SUPERSONIC FLOW

**Given structural criteria.**—According to the theory of linearized supersonic flow, the local surface pressure coefficient on an airfoil is given by

$$P = \frac{2}{\beta} y' \quad (\beta \equiv \sqrt{M_\infty^2 - 1})$$

For this approximation the basic differential equation (11b) becomes

$$y'^2 \frac{2}{\beta} = \lambda [(t/2)^n - y^n] \quad (17)$$

or, after solving for  $dx/dy$ ,

$$\sqrt{\frac{\lambda \beta}{2}} x = \int \frac{dy}{\sqrt{(t/2)^n - y^n}} \quad (18)$$

This can be put into a more convenient form by introducing the dimensionless variables  $X$ ,  $Y$ ,  $L$ , and  $H$  defined in the list of symbols, and eliminating  $\sqrt{\lambda \beta}$  by evaluating equation (18) at  $x = s$ . Between the leading edge and the first downstream position of maximum thickness  $dy/dx$  is positive while the dimensionless variables  $X$  and  $Y$  both vary from 0 to 1. Along the length of straight midsection  $Y = 1$ , while  $X$  varies from 1 to  $1 + L$ . Along the downstream portion of curved surface  $dy/dx$  is negative and  $Y$  varies from 1 to  $H$ , while  $X$  varies from  $1 + L$  to  $c/s$ . Consequently, equation (18) giving  $X$  as a function of  $Y$  becomes (with the convention that the sign of all radicals is positive)

$$X = \begin{cases} 1 - \frac{1}{k_n} \int_Y^1 \frac{dY}{\sqrt{1 - Y^n}} & \text{on surface facing upstream} \\ 1 + L + \frac{1}{k_n} \int_Y^1 \frac{dY}{\sqrt{1 - Y^n}} & \text{on surface facing downstream} \end{cases} \quad (19)$$

where the constant  $k_n$  depends only on  $n$  and is given by the definite integral

$$k_n = \int_0^1 \frac{dY}{\sqrt{1 - Y^n}} = \begin{cases} 2 & \text{for } n = 1 \\ \pi/2 & \text{for } n = 2 \\ 1.4023 \dots & \text{for } n = 3 \end{cases} \quad (20)$$

It may be noted here that integrals of the type occurring in equation (19) also occur at numerous places in the subsequent analysis. Such an integral, being a function of the

<sup>5</sup> It should be noted that the value  $n = 0$ , when substituted in the auxiliary integral, gives  $I = (t/2)^{-\sigma} = \text{constant}$ ; but this value cannot be used to obtain the solution for the case of a given thickness ratio because  $n = 0$  is incompatible with equation (13).

parameter  $n$  and the lower limit  $Y$ , can be evaluated either graphically or analytically. An analytical evaluation for the first three integer values of  $n$  yields

$$\int_Y^1 \frac{dY}{\sqrt{1-Y^n}} = \begin{cases} 2\sqrt{1-y} & \text{for } n=1 \\ \pi/2 - \arcsin Y & \text{for } n=2 \\ 3^{-1/4} F(k, \varphi) & \text{for } n=3 \end{cases} \quad (21)$$

where

$$k = \sin \frac{5\pi}{12} = 0.9659 \dots \quad \cos \varphi = \frac{\sqrt{3}-1+Y}{\sqrt{3+1-Y}}$$

The function  $F(k, \varphi)$  is the incomplete elliptic integral of the first kind of modulus  $k$  and amplitude  $\varphi$ . (A table of this function is given in reference 7, page 122.) For convenience the various formulas developed later are left in terms of the above integral; specialization to the individual functions indicated in equation (21) for a given  $n$  could be made in any subsequent formula if desired.

For linearized supersonic flow, equation (12) becomes

$$\begin{aligned} P_b &= P_1 + \left( y' \frac{\partial P}{\partial y'} \right)_1 \\ &= \frac{4}{\beta} \left( \frac{dy}{dx} \right)_1 \\ &= \frac{2(t/c)}{\beta(s/c)} \left( \frac{dY}{dX} \right)_1 \end{aligned}$$

or, on using the relation  $-k_n dX = dY/\sqrt{1-Y^n}$  which applies to the surface facing downstream (equation (9)), there is obtained

$$\frac{P_b \beta}{t/c} = \frac{2k_n \sqrt{1-H^n}}{(s/c)} \quad (22)$$

As defined earlier,  $H \equiv h/t$  is the optimum trailing-edge thickness expressed as a fraction of the maximum thickness.

Equation (13) can be written, in terms of  $X$  and  $Y$ , as

$$\frac{l}{s} = \frac{\sigma}{n} \left( \int_0^1 Y^n dX + l + \int_{1+L}^{c/s} Y^n dX \right) \quad (23a)$$

or, after specializing to linearized flow,

$$L \equiv \frac{l}{s} = \frac{\sigma}{nk_n} \left( \int_0^1 \frac{Y^n dY}{\sqrt{1-Y^n}} + k_n L + \int_H^1 \frac{Y^n dY}{\sqrt{1-Y^n}} \right) \quad (23)$$

Equations (22) and (23) can be put into more usable forms by noting from equation (19) that

$$\frac{c}{s} = 1 + L + \frac{1}{k_n} \int_H^1 \frac{dY}{\sqrt{1-Y^n}} \quad (24)$$

After some algebraic manipulation involving integration by parts and introduction of the definition  $B \equiv -P_b \beta / (t/c)$  there results from combining equations (22), (23), and (24),

$$B = \frac{2n(n+2-\sigma)\sqrt{1-H^n}}{(n-\sigma)(n+2)} \left[ k_n + \frac{2\sigma H \sqrt{1-H^n}}{n(n+2-\sigma)} + \int_H^1 \frac{dY}{\sqrt{1-Y^n}} \right] \quad (25)$$

and

$$L = \frac{2\sigma}{k_n(n-\sigma)(n+2)} \left( k_n + H \sqrt{1-H^n} + \int_H^1 \frac{dY}{\sqrt{1-Y^n}} \right) \quad (26)$$

These latter two equations are the final equations determining the optimum dimensionless trailing-edge thickness  $H$  and the optimum dimensionless length of straight midsection  $L$ . The corresponding equations involving the given value of  $I$  can be developed from equations (13), (22), (25), and (26) as follows:

$$\begin{aligned} \frac{I}{(t/2)^{n-\sigma}} &= \frac{l}{c} \frac{n}{\sigma} = \frac{s}{c} \left( L \frac{n}{\sigma} \right) = \frac{2k_n \sqrt{1-H^n}}{B} \left( L \frac{n}{\sigma} \right) \\ &= \frac{2}{n+2-\sigma} \left\{ \frac{k_n + H \sqrt{1-H^n} + \int_H^1 \frac{dY}{\sqrt{1-Y^n}}}{k_n + \frac{2\sigma H \sqrt{1-H^n}}{n(n+2-\sigma)} + \int_H^1 \frac{dY}{\sqrt{1-Y^n}}} \right\} \quad (27) \end{aligned}$$

This last equation determines  $H$  as a function of  $I/(t/2)^{n-\sigma}$ , or vice versa. It is to be noted from equations (24), (26), and (27) that the geometry of an optimum profile for given values of  $n$  and  $\sigma$  is determined solely by  $H$ , which, in turn, depends only on the base pressure parameter  $B$  (equation (25)).

**Given thickness ratio.**—Since the use of linearized theory provides a general solution in closed form of the basic equations (11b), (12), and (13), the optimum profile for a given thickness ratio can be obtained, according to considerations presented earlier, simply by letting  $n \rightarrow \infty$  in the general solution. Since  $Y$  is less than unity, it is evident that, for very large values of  $n$ ,

$$\int_Y^1 \frac{dY}{\sqrt{1-Y^n}} \rightarrow \int_Y^1 dY = 1 - Y, \quad \text{and } k_n \rightarrow 1.$$

Using equations (19) and (25), and noting that  $L=0$  for the present case, it follows that

$$X = \begin{cases} Y & \text{on surface facing upstream} \\ 2 - Y & \text{on surface facing downstream} \end{cases} \quad (28)$$

$$B = 2(2 - H) \quad (29)$$

$$\frac{s}{c} = 1/(2 - H) = 2/B \quad (30)$$

Equation (28) shows that the optimum surface has a discontinuity in slope at  $X=1$ , and that both segments make a common angle with the chord plane. Equation (29) provides the required relation between the base pressure parameter  $B$  and the optimum trailing-edge thickness. Equation (30) determines the position of maximum thickness. As  $H$  varies from 0 to 1 equation (29) covers only the range of  $B$  from 2 to 4. Within this range the above equations apply, and the optimum profile is of the type illustrated in figure 3. For the range of  $B$  from 0 to 2 the second possible solution discussed earlier, namely, a wedge profile, represents the optimum section. For values of  $B$  greater than 4 the

double-wedge airfoil with a sharp trailing edge is the optimum for a given thickness ratio.

It is remarked that the above solution also can be obtained quite easily by solving equations (14) and (15) directly, instead of employing the limiting process. This direct method can be used to determine the optimum profile in those cases where the general solution in terms of  $n$  and  $\sigma$  cannot readily be found. Such is the case when shock-expansion and similar higher-order theories are employed.

#### CALCULATION OF PRESSURE DRAG COEFFICIENT

**Given structural criteria.**—Since the dimensionless thickness distribution of an optimum profile is completely determined by the base pressure parameter, it is to be expected that the quantity  $\beta c_d/(t/c)^2$  also will depend only on  $B$ . From equation (1) and the definition of  $B$  it is seen that

$$\frac{\beta c_d}{(t/c)^2} = \frac{2\beta c}{t^2} \int_0^c P y' dx + B \frac{h}{t}$$

Substituting  $P=2y'/\beta$  and changing to the dimensionless variables  $X$ ,  $Y$ , and  $H$  yields

$$\frac{\beta c_d}{(t/c)^2} = \frac{c}{s} \int_0^{c/s} (dY/dX)^2 dX + BH$$

The integral can be expressed in terms of  $I/(t/2)^{n-\sigma}$  by noting that  $(dY/dX)^2 = k_n^2(1-Y^n)$  and that  $I/(t/2)^{n-\sigma} = (s/c) \int_0^{c/s} Y^n dX$ . There results for the pressure drag coefficient of the optimum profile in linearized flow:

$$\frac{\beta c_d}{(t/c)^2} = k_n^2 \frac{1 - [I/(t/2)^{n-\sigma}]}{(s/c)^2} + BH \quad (31)$$

Inasmuch as  $H$ ,  $s/c$ , and  $I/(t/2)^{n-\sigma}$  depend only on the base pressure parameter, the quantity on the left side of equation (31) also depends only on  $B$  for given values of  $n$  and  $\sigma$ .

It is of interest to compare the pressure drag of the theoretically optimum profile with that of more conventional sharp-trailing-edge profiles. According to linear theory the drag coefficient of a biconvex circular-arc airfoil  $(c_d)_{ca}$  of thickness  $t_{ca}$  is given by

$$\frac{\beta(c_d)_{ca}}{(t_{ca}/c)^2} = \frac{16}{3} \quad (32)$$

A calculation of the value of the auxiliary integral for a circular-arc profile  $(I_{ca})$  is readily made by substituting  $y=2(t_{ca}/c)x[1-(x/c)]$  in equation (2). It is found that

$$I_{ca} = \frac{2^{2n}(n!)^2}{(2n+1)!} (t_{ca}/2)^{n-\sigma}$$

By requiring that  $I_{ca}=I$  where  $I$  is the value of the auxiliary integral for the optimum profile of thickness  $t$  and position of maximum thickness at  $s/c$ , then equations (31) and (32) can be divided to yield

$$\frac{c_d}{(c_d)_{ca}} = \frac{k_n^2 \{1 - [I/(t/2)^{n-\sigma}]\} + BH(s/c)^2}{\frac{16}{3} (s/c)^2 \left\{ \frac{(2n+1)!}{2^{2n}(n!)^2} [I/(t/2)^{n-\sigma}] \right\}^{\frac{2}{n-\sigma}}} \quad (33)$$

This equation gives the ratio of the pressure drag of an optimum profile to that of a sharp-trailing-edge, circular-arc profile having an equal value for  $I$ . If the pressure drag coefficient of a double-wedge profile  $(c_d)_{dw}$  is used as a basis of comparison instead of a circular-arc profile, there results in a similar manner

$$\frac{c_d}{(c_d)_{dw}} = \frac{k_n^2 \{1 - [I/(t/2)^{n-\sigma}]\} + BH(s/c)^2}{4(s/c)^2 \{ (n+1)[I/(t/2)^{n-\sigma}] \}^{\frac{2}{n-\sigma}}} \quad (34)$$

It may be noted that the right side of equations (33) and (34) depend only on the base pressure parameter if the values of  $n$  and  $\sigma$  are given.

**Given thickness ratio.**—As noted earlier,  $k_n \rightarrow 1$  as  $n \rightarrow \infty$ . From equation (27) it follows that  $I/(t/2)^{n-\sigma} \rightarrow 0$ . By considering equations (29), (30), and (31) there results

$$\left[ \frac{\beta c_d}{(t/c)^2} \right]_{n=\infty} = 2B - \frac{B^2}{4} = 4 - H^2 \quad \text{for } 2 \leq B \leq 4 \quad (35)$$

Since  $[\beta c_d/(t/c)^2]_{ca} = 16/3$  and  $[\beta c_d/(t/c)^2]_{dw} = 4$ , it follows that

$$\frac{c_d}{(c_d)_{ca}} = \frac{3}{16} \left( 2B - \frac{B^2}{4} \right) = \frac{3}{16} (4 - H^2) \quad \text{for } 2 \leq B \leq 4 \quad (36)$$

and

$$\frac{c_d}{(c_d)_{dw}} = \frac{B}{2} - \frac{B^2}{16} = 1 - \frac{H^2}{4} \quad \text{for } 2 \leq B \leq 4 \quad (37)$$

These are the same two equations that would be obtained by passing equations (33) and (34) to the limit as  $n \rightarrow \infty$ . When  $B \leq 2$ , the optimum airfoil for a given thickness ratio, as previously discussed, is a wedge, for which  $\beta c_d/(t/c)^2 = 1+B$ ,  $c_d/(c_d)_{ca} = 3(1+B)/16$ , and  $c_d/(c_d)_{dw} = (1+B)/4$ . When  $B \geq 4$ , the optimum is a double wedge, for which  $\beta c_d/(t/c)^2 = 4$ ,  $c_d/(c_d)_{ca} = 3/4$ , and  $c_d/(c_d)_{dw} = 1$ .

If it is desired to compare the optimum profile with a corresponding sharp-trailing-edge profile on the basis of relative  $I$  for a given  $c_d$ , rather than on the basis of relative  $c_d$  for a given  $I$ , then the foregoing calculations can be applied by making only minor modifications. As noted earlier, the thickness distribution of the optimum profile having maximum  $I$  for a given  $c_d$  is the same as that of the optimum profile having a minimum  $c_d$  for a given  $I$ . By using the subscript  $s$  to denote a sharp-trailing-edge airfoil (e. g., biconvex, or double-wedge), and no subscript to denote the optimum profile, the relation

$$\left( \frac{I}{I_s} \right)_{c_d = \text{const.}} = \left( \frac{c_d}{c_d} \right)_{I = \text{const.}}^{\frac{n-\sigma}{2}}$$

can be deduced if it is remembered that  $I$  varies as the  $(n-\sigma)$  power of the thickness, and that the pressure drag in linearized theory varies as the square of the thickness. The above equation shows that in employing an optimum section the relative structural improvement that can be obtained for a given drag is related in a simple way to the relative drag reduction that can be obtained for a given structural requirement.

## RESULTS FOR LINEARIZED FLOW AND DISCUSSION

Significance and physical meaning of the base pressure parameter.—The determination of an optimum profile in linearized flow is greatly simplified by the fact that the dimensionless thickness distribution  $Y(x)$  depends only on the base pressure parameter  $B \equiv -P_b \beta / (t/c)$ , and not on the individual values of  $P_b$ ,  $M_\infty$ , or  $t/c$ .

Thus, although the Mach number, base pressure, and airfoil thickness ratio each indirectly affect the optimum airfoil profile, it is only necessary to know the value of  $B$  in order to determine the dimensionless thickness distribution ( $2y/t$ ) of the optimum airfoil section. Knowledge of both  $I$  and  $B$ , of course, is sufficient to determine  $t/c$  as well as the dimensionless distribution of thickness.

A simple physical interpretation of the base pressure parameter can be given if it is recalled that the basic means by which a thickened trailing edge reduces the over-all pressure drag is through a decrease in pressure foredrag at the expense of a smaller increase in base drag. Thus the optimum dimensionless distribution of thickness must depend essentially on the ratio of base drag to pressure foredrag. The base drag for a given  $H$  is proportional to  $(-P_b)(t/c)$ ; whereas the pressure foredrag for a given  $Y$  distribution is, according to linearized theory, proportional to  $(t/c)^2 / \sqrt{M_\infty^2 - 1}$ .

Hence,

$$\frac{\text{base drag}}{\text{pressure foredrag}} \sim \frac{-P_b(t/c)}{(t/c)^2 / \sqrt{M_\infty^2 - 1}} = \frac{-P_b \sqrt{M_\infty^2 - 1}}{t/c} = B$$

or, in words, the base pressure parameter is proportional to the ratio of base drag to pressure foredrag.

Condition under which optimum profile has a blunt trailing edge.—From equation (25) it is easy to deduce the condition under which the optimum airfoil will have a blunt trailing edge. The critical condition is obtained by setting  $H=0$ . This determines a particular value of  $B$ , say  $\bar{B}$ .

$$\bar{B} = \frac{4nk_n(n+2-\sigma)}{(n-\sigma)(n+2)} = \begin{cases} 8 & \dots \text{ for } n=1, \sigma=0 \\ 6.283 & \dots \text{ for } n=2, \sigma=0 \\ 5.609 & \dots \text{ for } n=3, \sigma=0 \\ 9.425 & \dots \text{ for } n=2, \sigma=1 \\ 6.730 & \dots \text{ for } n=3, \sigma=1 \\ 4 & \dots \text{ for } n=\infty, \sigma \text{ finite} \end{cases} \quad (38)$$

A lower value of  $B$  would correspond, for example, to a lower base drag, hence the physical significance of  $\bar{B}$  can be stated quite simply: the optimum airfoil has a blunt trailing edge for  $B < \bar{B}$ ; whereas it has a sharp trailing edge for  $B \geq \bar{B}$ .

Comparison with results of other investigations.—As a partial check on the equations developed, several limiting cases can be obtained by specializing to particular values of  $n$ ,  $\sigma$ , and  $H$ . First, if the base pressure coefficient is zero, corresponding either to zero base drag or else infinite Mach number, then  $B=0$ . From equation (25) it follows that  $H=1$ . In other words, the optimum profile for  $P_b=0$  has its maximum thickness at the trailing edge. If the Mach number is finite and the base drag zero, then this result

checks simple physical considerations. If the Mach number is infinite (for which  $B=0$  even if a vacuum exists at the base), then this result checks the qualitative consideration of Saenger referred to in the introduction.

A second limiting case that easily can be checked may be obtained by considering only the auxiliary conditions of given stiffness of sharp-trailing-edge profiles. The appropriate results are obtained by setting  $\sigma=0$  and  $H=0$ . From equation (26) it follows that  $l=0$ . From equations (19) and (21) it is seen that the optimum sharp-trailing-edge profile is a doubly symmetric profile, each side of which is comprised of the arc of a parabola for  $n=1$ , the arc of a trigonometric sine function for  $n=2$ , and the arc of an elliptic sine function for  $n=3$ ; these are the results obtained previously by Drouge.

Summary curves of the principal results.—In figure 4 the optimum dimensionless trailing-edge thickness  $H$  is plotted as a function of the base pressure parameter  $B$ . Each curve in this figure is obtained by substituting the indicated values of  $n$  and  $\sigma$  in equation (25). It is to be remembered that the curve consisting of three straight-line segments, corresponding to  $n=\infty$  and  $\sigma=\text{finite}$ , represents the auxiliary condition of a given thickness ratio. The other values of  $n$  and  $\sigma$  represent the various structural criteria listed in the table presented earlier.

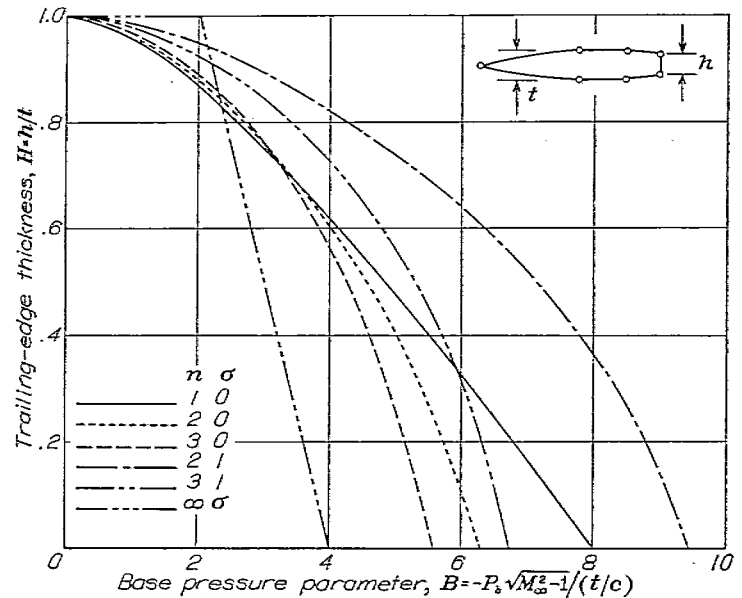


FIGURE 4.—Optimum trailing-edge thickness for linearized supersonic flow.

The location of the optimum position of maximum thickness  $s/c$ , as determined by equations (24) and (26), is plotted in figure 5 as a function of  $B$ . The values of  $n$  and  $\sigma$  used here are the same as in figure 4. Comparing these two figures it can be seen that, as would be expected, the optimum position of maximum thickness moves steadily rearward as the optimum trailing-edge thickness is increased.

Curves relating the value of  $I$  to the base pressure parameter are shown in figure 6. These curves represent equation (27). Since  $I$  is related to the optimum length of straight midsection through equation (13), the ordinate in this figure represents either of the two equal quantities,  $I/(t/2)^{2-\sigma}$  or  $nl/\sigma c$ . Figure 6, therefore, can also be used to

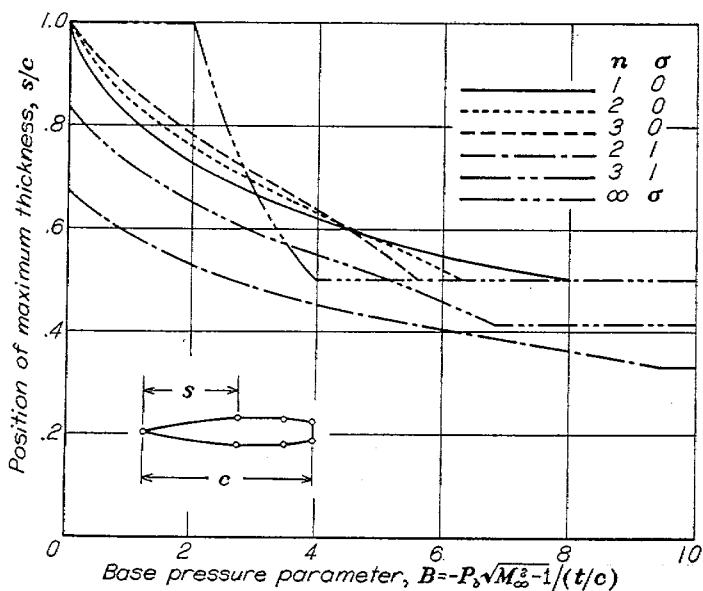


FIGURE 5.—Optimum position of maximum thickness for linearized supersonic flow.

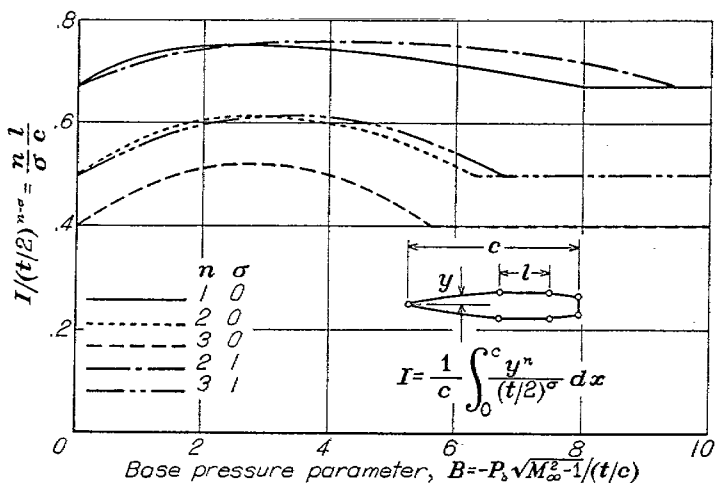
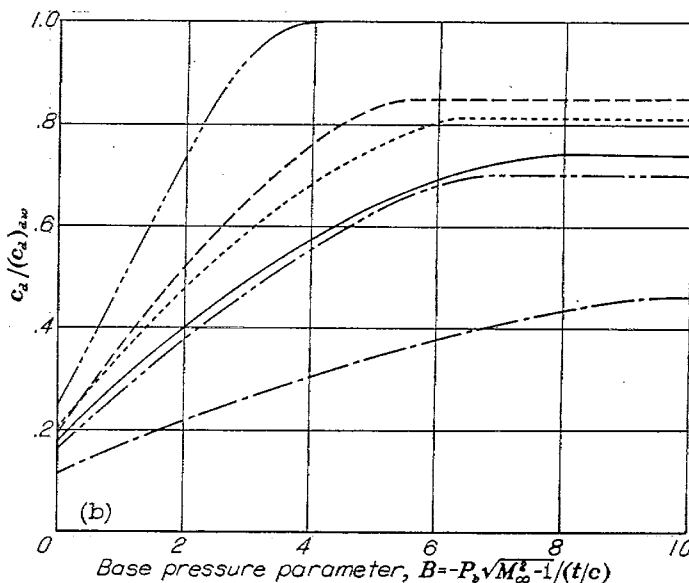
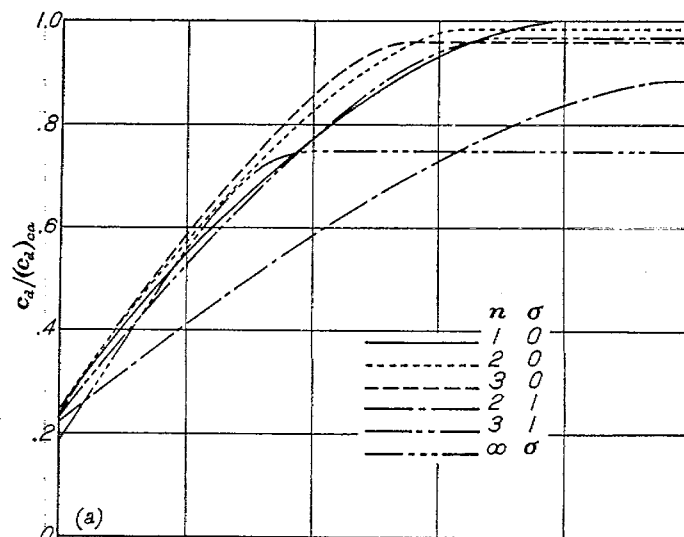


FIGURE 6.—Curves relating  $I$  and  $l$  to the base pressure parameter for linearized supersonic flow.

determine  $l/c$  in those cases where  $\sigma$  is not zero. If  $\sigma$  is zero, then  $l$  is zero, as noted before.

In figure 7 the two quantities  $c_d/(c_d)_{ca}$  and  $c_d/(c_d)_{dw}$  are plotted as a function of  $B$  for various values of  $n$  and  $\sigma$ . Depending on the value of  $B$ , it is apparent that the pressure drag of the optimum profile may be anywhere from a few percent to as much as 75 percent less than the pressure drag of an equivalent circular-arc sharp-trailing-edge airfoil. The structural criterion for which the greatest drag difference exists is that of a given bending strength of a thin-skin structure ( $n=2, \sigma=1$ ). The curves of figure 7 (b) clearly illustrate the high drag of a double-wedge profile when it is compared to the optimum profile on the basis of a given structural requirement. These curves also illustrate that the relative drag reduction of the optimum airfoil for the condition of a given thickness ratio is much less than the corresponding reductions for the various conditions of given structural requirements.

**Method of determining an optimum profile from experimental base pressure data.**—The experiments of reference 8 have shown that the base pressure of airfoils in supersonic

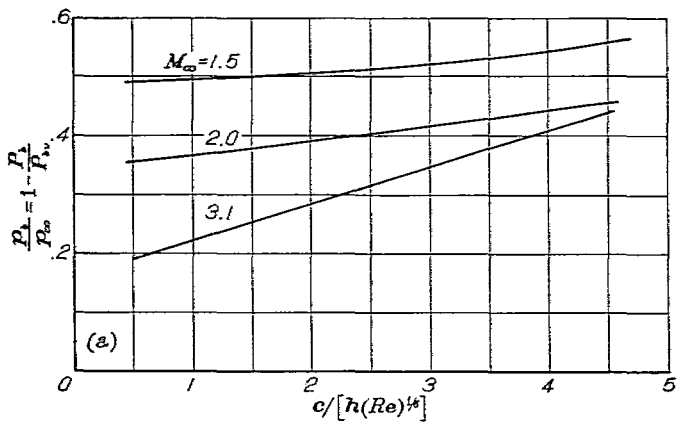


(a) Drag of optimum relative to biconvex circular-arc airfoils.  
(b) Drag of optimum relative to double-wedge airfoils.

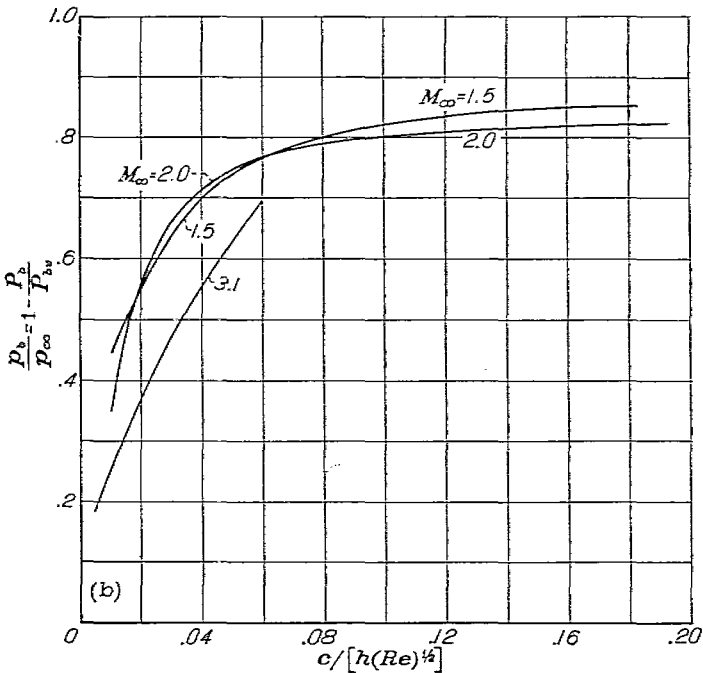
FIGURE 7.—Drag of optimum airfoils as compared to the drag of two different sharp-trailing-edge airfoils in linearized supersonic flow. Comparison made on the basis of equal values for the auxiliary integral.

flow depends primarily on the trailing-edge thickness, Reynolds number, and type of boundary-layer flow. The base pressure generally does not depend significantly on the shape of the airfoil profile upstream of the trailing edge. Figure 8 presents summary correlation curves (taken from reference 8) showing the dependence of base pressure on the parameters  $c/[h(Re)^{1/5}]$  and  $c/[h(Re)^{1/2}]$ , which are approximately proportional to the ratio of boundary-layer thickness to trailing-edge thickness for turbulent and laminar flow, respectively. Since the optimum profile depends on the base pressure, which, in turn, depends on the trailing-edge thickness of the optimum profile, the value of  $B$  is not known initially. For this reason the process of determining an optimum profile from the experimental data of figure 8 involves several steps:

(1) For an arbitrarily selected value of  $t/c$ ,  $B$  is computed as a function of  $H$  using the proper experimental value of base pressure for each  $H$ .



(a) Turbulent.



(b) Laminar.

FIGURE 8.—Average values of base pressure from experiments of reference 8.

(2) A plot of  $H$  versus  $B$  is superposed on figure 4. The point of intersection with the existing curve for the particular combination of  $n$  and  $\sigma$  in question determines optimum values of  $H$  and  $B$  for the particular  $t/c$  selected.

(3) Knowing  $t/c$ ,  $H$ , and  $B$  from (1) and (2),  $I$  is calculated from equation (27).

(4) The above process is repeated for several values of  $t/c$ . Interpolation for the desired value of  $I$  then yields the values of  $t/c$ ,  $H$ , and  $B$  of the optimum profile. The optimum value of  $B$  yields the optimum values of  $s/c$  and  $l/c$ . Equations (19) and (21) yield the basic shape of the curved portions of the desired airfoil.

The results of applying steps (1) and (2) for a thickness ratio of 0.06, a Mach number of 3, and a turbulent boundary layer at  $Re=10^7$ , are shown in figure 9. It is seen that the optimum trailing-edge thickness varies between  $0.12t$  and  $0.67t$  for the different combinations of  $n$  and  $\sigma$ . The corresponding pressure drag reduction compared to a biconvex airfoil having the same value for the auxiliary integral varies between 6 and 29 percent, whereas compared to a double-wedge

airfoil the corresponding pressure drag reduction varies between 1 and 63 percent.

The effect of Mach number on the optimum profile for  $t/c=0.06$ ,  $n=1$ ,  $\sigma=0$ , and turbulent flow at  $Re=10^7$ , is shown in figure 10. For  $M_\infty=5$  an estimated value of  $p_0/p_\infty=0.15$  was employed since experimental base pressure data are not yet available at this Mach number. For  $M_\infty=\infty$  and  $M_\infty=1$ , it is not necessary to know the base pressure to determine the optimum profile with linear theory. A large effect of Mach number on the optimum profile, particularly at Mach numbers above about 3, is evident from figure 10. The effect of airfoil-thickness ratio on the geometry of the optimum profile also is large, as illustrated in figure 11. (For the case  $t/c=0.02$  in this latter figure, it was necessary to extrapolate the experimental base-pressure curves of fig. 8 (a) in order to estimate the base pressure.) The trends illustrated in figures 10 and 11 can be explained from elementary physical consideration if it is recalled that  $B$  corresponds to the ratio of base drag to pressure foredrag. Thus,  $H$  approaches unity as  $M_\infty$  approaches unity because the pressure foredrag in linear theory approaches infinity while the base drag remains finite. Moreover,  $H$  also approaches unity as  $M_\infty$  approaches infinity because the base drag, which is approximately proportional to  $1/M^2$ , becomes small compared to the pressure foredrag, which in linear theory becomes proportional to  $1/M$ . By the same token,  $H$  approaches unity for very thick airfoils because the base drag, proportional to  $t/c$ , again becomes small compared

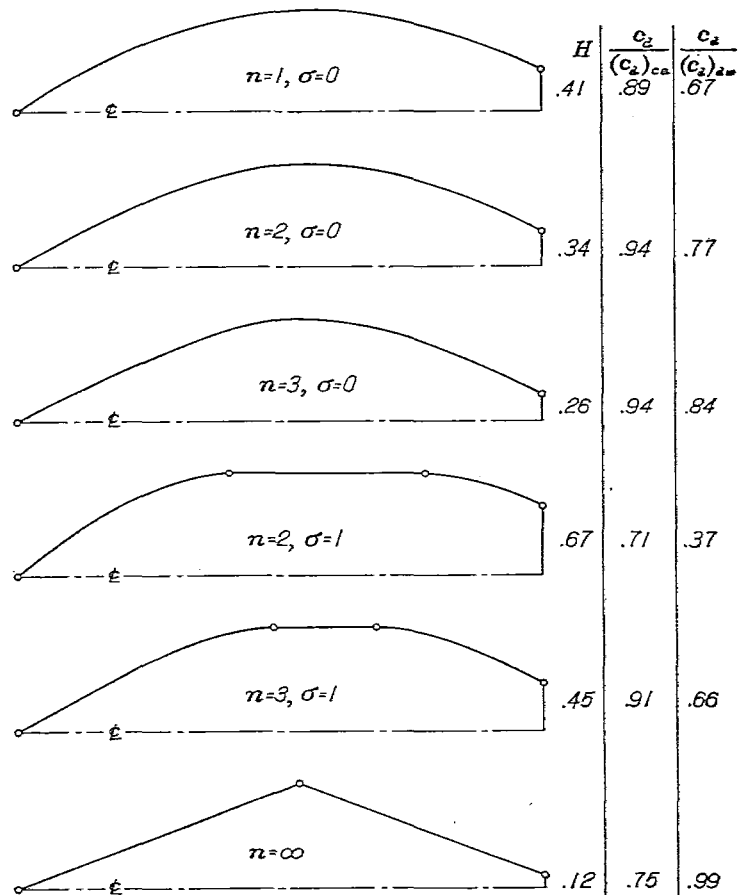


FIGURE 9.—Examples illustrating the effect of auxiliary condition on the optimum profile; linearized flow, vertical scale expanded,  $M_\infty=3$ ,  $t/c=0.06$ , turbulent flow at  $Re=10^7$ .

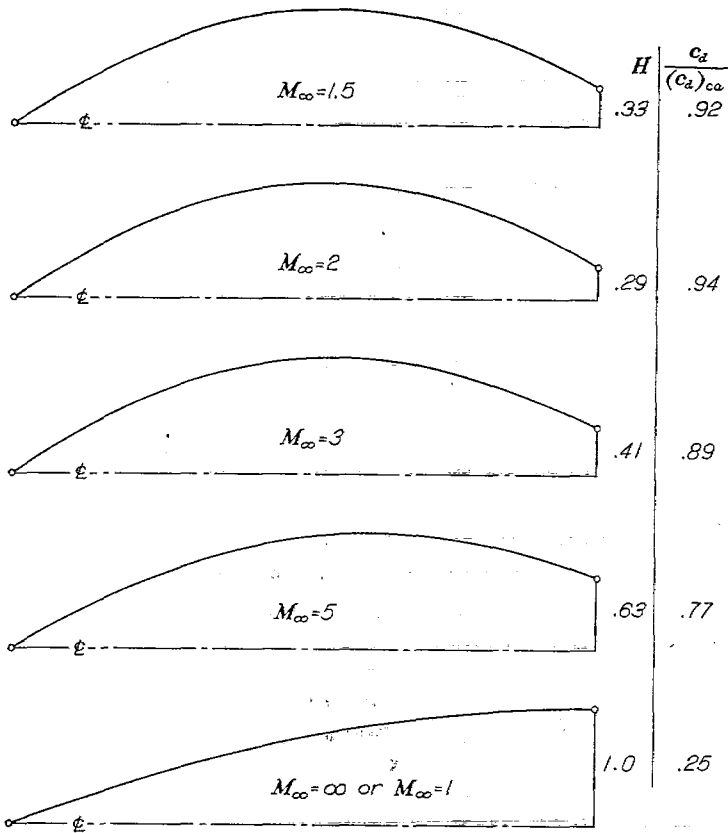


FIGURE 10.—Examples illustrating the effect of Mach number on the optimum profile linearized flow, vertical scale expanded,  $n=1$ ,  $\sigma=0$ ,  $t/c=0.06$ , turbulent flow at  $Re=10^7$ .

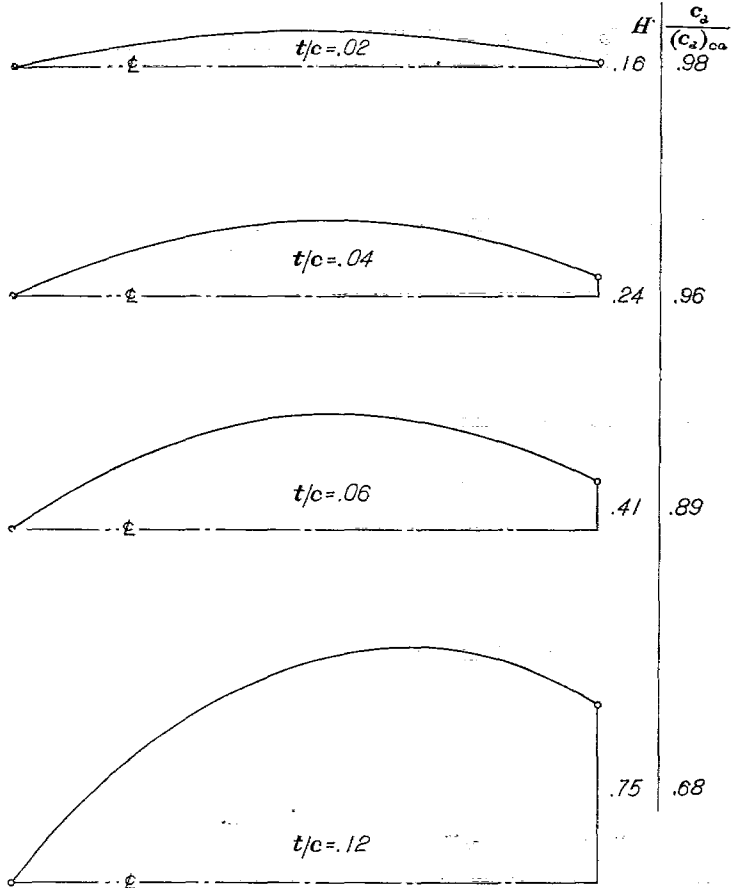


FIGURE 11.—Examples illustrating the effect of airfoil thickness ratio on the optimum profile; linearized flow, vertical scale expanded,  $n=1$ ,  $\sigma=0$ ,  $M_\infty=3$ , turbulent flow at  $Re=10^7$ .

to the pressure foredrag, which in linear theory is proportional to  $(t/c)^2$ .

Reynolds number has an important effect on the optimum airfoil profile if the boundary layer is laminar. (See fig. 12.) This is because the base pressure depends markedly on Reynolds number for laminar flow. For turbulent flow the corresponding dependence is seen to be considerably less, and the optimum trailing-edge thickness is seen to be much less than for laminar flow.

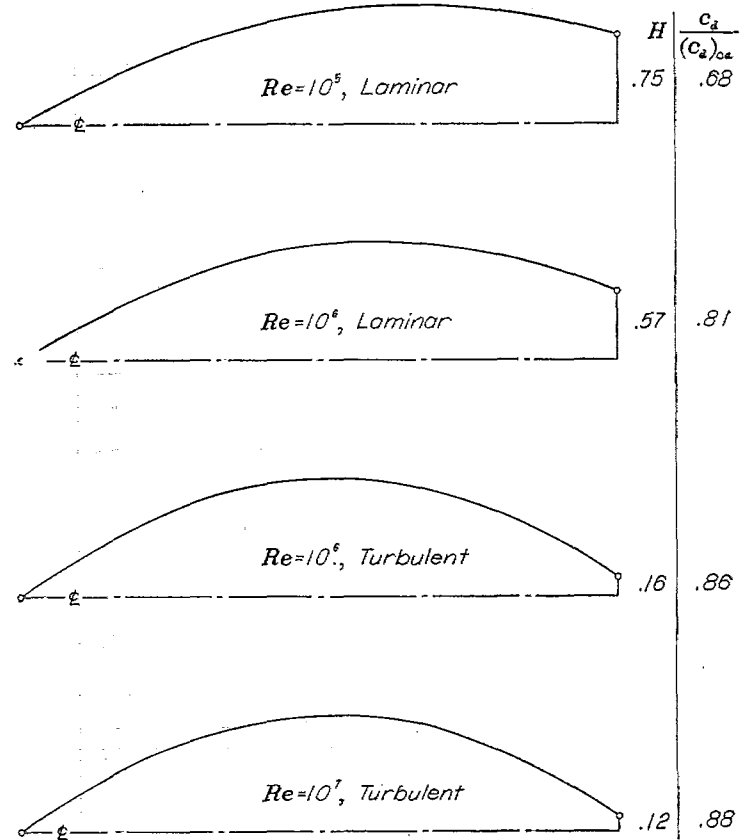


FIGURE 12.—Examples illustrating the effect of Reynolds number and type of boundary-layer flow on the optimum profile; linearized flow, vertical scale expanded,  $n=1$ ,  $\sigma=0$ ,  $M_\infty=2$ ,  $t/c=0.04$ .

CONCLUDING REMARKS

The general method presented for computing the profile shape having minimum pressure drag at zero lift has been developed for the auxiliary condition that

$$I \equiv \frac{1}{c} \int_0^c [y^n / (t/2)^\sigma] dx$$

is constant. For a given airfoil theory, the determination of an optimum profile under this condition involves the simultaneous solution of equations (11), (12), and (13), which are general in that the surface pressure coefficient  $P(y')$  and the parameters  $n$  and  $\sigma$  are arbitrary. Such generality is useful since it allows either linear theory, second-order theory, or shock-expansion theory to be used in determining the optimum profile for a number of practical auxiliary conditions such as prescribed bending strength or given torsional stiffness. As an illustration of the method, a solution has been developed in detail using linearized flow, that is, using the expression  $P=2y'/\sqrt{M_\infty^2-1}$ . In this

simple case a complete solution in closed form is obtained for the thickness distribution of the optimum profile.

The principal result of the analysis for linear supersonic flow is that the dimensionless thickness distribution of the optimum profile depends only on the single parameter  $B \equiv -P_b \sqrt{M_\infty^2 - 1} / (t/c)$ . This parameter has been termed the base pressure parameter, and has a simple physical significance in that it is proportional to the ratio of base drag to pressure foredrag. The dependence of an optimum profile in linear flow on one parameter only enables summary curves to be plotted showing all principal results as a function of  $B$  (figs. 4, 5, 6, and 7). The optimum dimensionless trailing-edge thickness increases if either the base pressure is increased, the airfoil-thickness ratio is increased, or the Mach number is increased to very high values.

At low supersonic Mach numbers the theoretical results obtained are questionable since the assumptions of linearized airfoil theory break down as the Mach number approaches unity. The results can be applied safely only to cases where linear theory satisfactorily predicts the pressure foredrag. Although at high supersonic Mach numbers the results obtained under the assumption of linearized flow also would not be expected a priori to be of quantitative value, they predict, nevertheless, the correct result that the optimum trailing-edge thickness for infinite Mach number is equal to the maximum airfoil thickness. In view of this exact agreement in the extreme case, it is conjectured that the linear theory fortuitously may provide a reasonable estimate of the optimum trailing-edge thickness for any supersonic Mach number not close to unity. As regards the optimum profile shape forward of the base, however, such fortuitous conditions cannot be expected,

since the linearized approximation at high Mach numbers overestimates the suction forces and underestimates the positive pressure forces. This causes the calculated optimum profile to have too large a leading-edge angle, a position of maximum thickness too far forward, and too small an inclination of the surface behind the position of maximum thickness. (In reference 9 some calculations using second-order theory are presented which illustrate this effect on the optimum sharp-trailing-edge profile for the auxiliary condition of a given thickness ratio.)

Because the optimum profile, by definition, has the least pressure drag possible under given conditions, small changes in profile shape would result in second-order changes in drag. This allows some flexibility in modifying the theoretically optimum profile to more closely suit individual design requirements, and means that it is not important to rigorously adhere to the exact parabolic, trigonometric-sine, or elliptic-sine contour (provided, of course, that the end points of the modified contour are located approximately in the optimum positions). It is important to adhere reasonably close to the calculated optimum trailing-edge thickness, since this quantity can greatly affect the drag. In particular, a trailing-edge thickness considerably greater than the optimum should not be used. Excessive trailing-edge thickness at low and moderate supersonic Mach numbers can result in an excessive increase in drag.

AMES AERONAUTICAL LABORATORY,  
NATIONAL ADVISORY COMMITTEE FOR AERONAUTICS,  
MOFFETT FIELD, CALIF., October 3, 1950.

## APPENDIX

## NOTE REGARDING DISCONTINUANCE CHANGE IN SLOPE OF AN OPTIMUM PROFILE

In the general analysis of optimum profiles for a given thickness ratio it was found that the function  $y'^2 \frac{\partial P}{\partial y'}$  necessarily was constant along each straight segment of the profile (equation (14)). No information was obtained, however, about the relative value of this constant for the two segments. The required information can readily be obtained by considering the change in drag due to a change only in position of maximum thickness, that is, a change in slope of both straight surfaces illustrated in figure 3 with no change in  $t$  or  $h$ . Using subscripts  $u$  and  $d$  to denote surfaces facing upstream and downstream, respectively, it follows that

$$\begin{aligned} \delta c_d &= \delta(c_d)_u + \delta(c_d)_d \\ &= t \left( \frac{\partial P}{\partial y'} \right)_u \delta y'_u + (t-h) \left( \frac{\partial P}{\partial y'} \right)_d \delta y'_d \end{aligned}$$

Since  $y'_u = t/s$  and  $y'_d = (t-h)/(c-s)$ , the minimizing of  $c_d$  requires that

$$\begin{aligned} \delta c_d = 0 &= - \left( \frac{\partial P}{\partial y'} \right)_u \frac{t^2}{s^2} \delta s + \left( \frac{\partial P}{\partial y'} \right)_d \frac{(t-h)^2}{(c-s)^2} \delta s \\ 0 &= \delta s \left[ y'^2_u \left( \frac{\partial P}{\partial y'} \right)_u - y'^2_d \left( \frac{\partial P}{\partial y'} \right)_d \right] \end{aligned}$$

Thus  $y'^2 \frac{\partial P}{\partial y'}$  must be continuous at the corner—a result which was used without proof in the general analysis. It may be noted that an alternate proof of this result can be obtained in an extremely easy way from the following known result of the calculus of variations: The Weierstrass E-function is continuous at the point of discontinuity on a boundary. The E-function in the present case is  $y'^2 \frac{\partial P}{\partial y'}$ .

For auxiliary conditions other than a given thickness ratio it was tacitly assumed in the analysis that the optimum surface everywhere had a continuous slope. This assumption

also requires some justification. It is shown in the calculus of variations that at all points of free variation it is necessary for  $\frac{\partial f}{\partial y'}$  to be continuous. For the present problem this means that  $P + y' \frac{\partial P}{\partial y'}$  must be continuous at all such points. According to linear theory,  $P + y' \frac{\partial P}{\partial y'} = \frac{4}{\beta} y'$ , hence, within the scope of linear theory, the surface slope  $y'$  is continuous at all points of free variation. For shock-expansion theory  $\frac{\partial P}{\partial y'}$  is positive, and a corner would cause a discontinuous decrease in  $P$ ,  $y'$ , and  $P + y' \frac{\partial P}{\partial y'}$ ; hence, also within the scope of shock-expansion theory the surface slope of the optimum profile is continuous at all points of free variation. This justifies the assumption of continuous slope employed in the general analysis for auxiliary conditions other than a given thickness ratio.

## REFERENCES

1. Drougge, Georg: Wing Sections with Minimum Drag at Supersonic Speeds. Rep. No. 26, Aero. Res. Inst. of Sweden (Stockholm), 1949.
2. Ferri, Antonio: Experimental Results with Airfoils Tested in the High-Speed Tunnel at Guidonia. NACA TM 946, 1940.
3. Chapman, Dean R.: Base Pressure at Supersonic Velocities. California Institute of Technology Thesis, 1948.
4. Saenger, Eugen: Raketen-Flugtechnik. Verlag von R. Oldenbourg, Munchen und Berlin, 1933.
5. Ivey, H. Reese: Notes on the Theoretical Characteristics of Two-Dimensional Supersonic Airfoils. NACA TN 1179, 1947.
6. Smeit, R.: Problems of Missiles at Extreme Speeds. Naval Ordnance Laboratory Rep. No. 1131, Symposium on Ordnance Aeroballistics, June 1949.
7. Peirce, B. O.: A Short Table of Integrals. Third revised edition, Ginn and Company, N. Y., 1929.
8. Chapman, Dean R.; Wimbrow, William R., and Kester, Robert H.: Experimental Investigation of Base Pressure on Blunt-Trailing-Edge Wings at Supersonic Velocities. NACA TN 2611, 1951.
9. Ferri, Antonio: Elements of Aerodynamics of Supersonic Flows. The MacMillan Company, New York, 1949, pp. 133-136.